DOI: 10.1002/chem.201000772

VIP

# Twist Ferrocene Wires from Self-Assembly of Chiral Rod–Coil Organometallics

**Tz-Feng Lin,[a] Rong-Ming Ho,*[a] Chien-Hung Sung,[b] Ming-Shou Ho,[b] and Chain-Shu Hsu*[b]**

Inspired by research on organometallics, the incorporation of transition metals into organic derivatives through covalent attachment has become a mature field. Because of improvements in synthesis, the ferrocene-based moiety is now a well-known organometallic moiety.[1] Tunable ferrocene residues provide an attractive method to expand the range of properties. By taking advantage of self-assembly, various self-assembled organometallic morphologies including spheres, cylinders, vesicles, and lamellae with nanoscale iron-rich microdomains can be used in applications such as switches, transistors, and sensors for integration into microelectronic technology.[2] Also, ordered nanostructures transform into semiconducting materials after oxidation and yield iron-rich magnetic ceramics after pyrolysis treatment.[3]

Helical morphologies can be obtained from the self-assembly of chiral supramolecules such as chiral liquid crystals,[4] folded oligomers,[5] chiral counterions,[6] chiral dendrimers,[7] dendron rod–coils,[8] chiral homopolymers,[9] chiral block copolymers,[10] and chiral discotic molecules.[11] In our previous studies, the self-assembly of a series of chiral Schiff based rod–coil amphiphiles was systematically examined.[12] The self-assembled helical superstructures could be induced by chiral sugar, and a morphological transformation from helical to platelet-like morphology was driven by simply increasing the hydrophobic chain length at the chain end of the chiral rod–coil amphiphiles. The helical morphology results from the steric-hindrance effect of the chiral sugar packing in the self-assembly.

Herein we aim to create iron-rich spiral superstructures by taking advantage of the self-assembly of chiral Schiff based rod–coil molecules that are end-capped with ferrocene (namely, chiral rod–coil organometallics). Figure 1 demonstrates the chemical structure of a chiral rod–coil organometallic, 4-(11-Ferrocenoyloxy-undecanyl-1-oxy)-benzylideneaminophenyl-α-D-glucopyranside (FC11). Corresponding synthetic routes and characterization of the chiral rod–coil organometallics are described in detail in the Supporting Information and are in full agreement with the suggested chemical structure. As found, sugar moieties can serve as a chiral source for helical twisting and bending. The rod segment is the mesogenic unit responsible for liquid-crystalline behavior in the self-assembly process. The alkoxyl chain end is capped by a ferrocenyl group through the esterification of the aliphatic tail with ferrocene carboxylic acid. Consequently, twist superstructures with a ferrocene core are expected to be obtained through the self-assembly of the chiral rod–coil organometallics. The self-assembled superstructure can then be utilized as a template to form an iron-rich superstructure after pyrolysis, resulting in promising applications in devices.

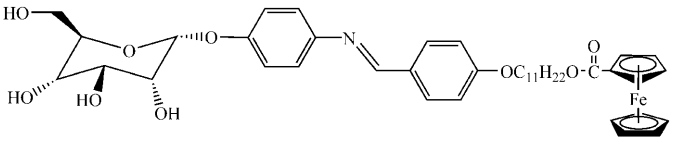


Figure 1. Chemical structure of the chiral rod–coil organometallics, FC11.

Thermal analysis suggests that FC11 possesses enantiotropic liquid-crystalline properties (see Figures S1 and S2 in the Supporting Information). To identify the corresponding

[a] Dr. T.-F. Lin, Prof. Dr. R.-M. Ho
Department of Chemical Engineering
National Tsing-Hua University, Hsinchu, 30013 (Taiwan)
Fax: (+886) 3-5715408
E-mail: rmho@mx.nthu.edu.tw

[b] Dr. C.-H. Sung, Dr. M.-S. Ho, Prof. Dr. C.-S. Hsu
Department of Applied Chemistry
National Chiao-Tung University, Hsinchu, 30010 (Taiwan)
Fax: (+886) 3-5131523
E-mail: cshsu@mail.nctu.edu.tw

Supporting information for this article is available on the WWW under http://dx.doi.org/10.1002/chem.201000772. The chemical structures, experimental data, characterization analyses, polarized-light microscopy images, and differential scanning calorimeter thermograms are included.

   

liquid-crystalline phase transformation during cooling, X-ray scattering experiments were performed from isotropic melts to preset temperatures. As illustrated in Figure 2, well-ordered diffraction peaks at a characteristic ratio of 1:2 are found when the temperature is below 120 °C. The layer-to-layer d spacing ($d$) appears to be 6.40 nm according to the primary scattering peak of the X-ray results. On the basis of the FC11 chain conformation, the extended chain length ($l$) is estimated as approximately 3.36 nm through HyperChem 7 molecular simulation with an OPLS force field. As a result, we suggest that instead of interdigitated layer-to-layer molecular packing, the chiral rod–coil organometallics adopt a parallel type of molecular chain packing. Furthermore, the broadening peak above 120 °C is attributed to electron density contrast between ferrocene and organic microdomains at temperatures above the isotropic melting temperature.

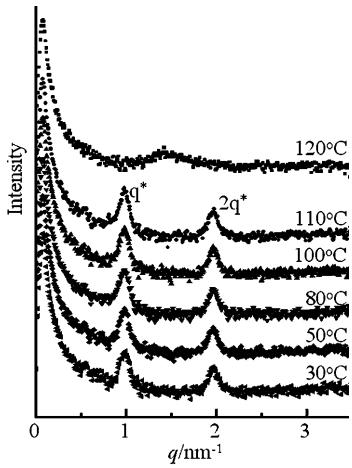


Figure 2. X-ray scattering profiles of FC11 examined at different temperatures by cooling from an isotropic melt.

The self-assembly of the chiral rod–coil organometallic material was carried out in dilute aqueous solution with FC11 (1 mg) dissolved in THF (1 mL) by introducing distilled water (9 mL) to induce aggregation. After sufficient time for aggregation, a drop of the mixture was transferred to a carbon-coated film for TEM analysis. As shown in Figure 3a (see Figure S3 in the Supporting Information for a complementary image), self-assembled FC11 superstructures with a clear fibrous texture can be recognized. The dark regions correspond to ferrocene microdomains owing to the mass-thickness contrast and the bright regions are the microdomains of the chiral Schiff based rod–coil segment. As estimated, the average diameter of the fibrous texture is 7 nm and the core diameter of the ferrocene microdomain is approximately 2 nm. The observed corona and core sizes are in line with the molecular sizes of the FC11. To examine the self-assembled superstructure further, platinum was shadow-evaporated onto the sample. As shown in Figure 3b, not only the fibrous bundle, but every wirelike twist can be clearly identified on the basis of its surface topograghy.

On the basis of the morphological observation and structural analyses, the self-assembled morphologies arise from aggregation of FC11 molecules to hierarchical superstructures through liquid-crystalline behavior in solution.[12a] UV/Vis and circular dichroism (CD) spectroscopy measurements were carried out to elucidate the conformational chirality of the chiral rod–coil organometallics in THF solution (see Figure S4 in the Supporting Information). The UV/Vis spectra demonstrates the maximum absorption of the π–π* and n–π* transition for FC11 at around 280 nm and 330 nm. The corresponding positive Cotton effect around the corresponding wavelength indicates a helical packing arrangement of the chiral rod–coil organometallics as a microdomain. As illustrated in Figure 3c, the self-assembled FC11 superstructure is constructed of several wirelike twists. Its internal structure appears as a smectic-like bilayer that has parallel molecular chain packing according to the X-ray scattering experiments and theoretical simulation prediction. Note that helical architectures might be formed from the self-assembly of achiral liquid-crystalline molecules through head-to-head twisted dimers and bent-core induced chirality (i.e., a molec-

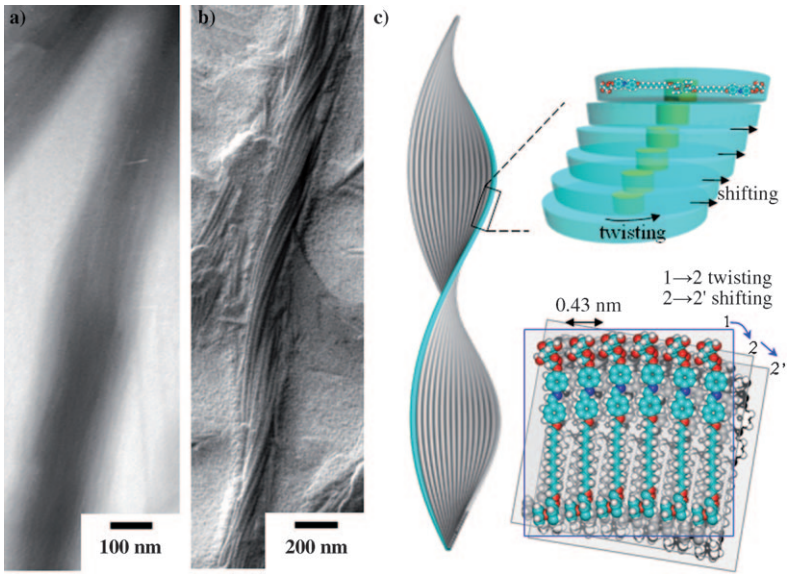


Figure 3. TEM micrographs of self-assembled FC11 from solution at ambient temperature a) without and b) with Pt shadowing. The dark regions in (a) correspond to ferrocene microdomains. The morphology in (b) shows the topography of the self-assembled texture. c) A schematic illustration of the formation of hierarchical superstructures from the self-assembly of chiral rod–coil organometallics.

  

ular shape effect).[13] In our case, the chiral effect (i.e., the steric-hindrance effect) of the sugar moiety gives rise to the twisting and shifting forces for the stacking of neighboring circular plates. Consequently, a dense core of the iron-rich microdomain is thus formed in the center of the circular plate because of the strong metal coordination of the ferrocene moiety and its incompatibility with water. A spiral staircase-like architecture is represented as connecting circular plates to show the helical packing arrangement of the building blocks.[14] According to the estimated periphery of the fibrous texture and the calculated width of single chiral rod–coil organometallics (approximately 0.43 nm), it is composed of about fifty chiral rod–coil organometallics aggregated into a basal circular plate that develops into the formation of the self-assembled FC11 superstructures, which are several micrometers long.

In an attempt to orient the self-assembled morphology of chiral rod–coil organometallics, a 1 T external magnetic field was used for the self-assembly process. The molecular director of the chiral rod–coil organometallics follows the direction of the magnetic field owing to its intrinsic dielectric constant. The self-assembled superstructures thus appear as an anisotropic aligned pattern over long distances (see Figure S5 in the Supporting Information). Pyrolysis was performed at a heating rate of 1 °C min$^{-1}$ under an $N_2$ atmosphere from room temperature to a final temperature of 600 °C. During the pyrolysis procedure, the organometallic microdomains transform into a collection of inorganic arrays as shown in Figure 4. Similar pyrolysis of ferrocene in

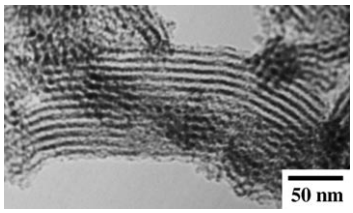


Figure 4. TEM micrograph from templates of self-assembled FC11 after pyrolysis

a self-assembled superstructure with polyferrocenylsilane cores and polyisoprene coronas has been reported in the form of micelles.[15] As a result, the superstructure resulting from the self-assembly of chiral rod–coil organometallics works as a template for the formation of twist metallic wires. The observed corona and core sizes of the twist metallic wire correspond to the theoretical molecular size of the FC11 and the results from Figure 3a, which indicate a twist fibrous superstructure with a ferrocene core (i.e., twist ferrocene wires).

In conclusion, we have described the synthesis and characterization of chiral rod–coil organometallics (FC11) that develop into ferrocene iron-rich spiral superstructures through self-assembly. This fundamentally new self-assembled FC11 superstructure is a fabrication technology that acts as a template for the formation of twist ferrocene wires. Such wires will contribute to the development of microelectronic organic–inorganic functional devices.[16] Also, the well-defined building blocks of ferrocene-based derivatives play an important role in dynamic responsive displays as well as in biological systems that are stimulated by external fields.[17]

## Experimental Section

**Structural determination**: To study the helical hierarchical superstructures that are driven by a chiral entity, the self-assembly of chiral rod–coil organometallics were carried out in dilute solution (THF/$H_2O$, 9:1 mL). After sufficient time for aggregation process to occur, a drop of the mixture was transferred to a carbon-coated film for TEM observations. Bright-field TEM images were performed on a JEOL TEM-1200 CXII transmission electron microscope at an accelerating voltage of 120 kV. UV/Vis absorption spectra and CD spectroscopy measurements were recorded on a Hitachi U-3300 spectrophotometer and JASCO J-720 spectrophotometer in quartz tubes, respectively. The spectroscopic experiments were carried out in THF solutions ($1\times10^{-4}$ M). Temperature-dependent X-ray scattering experiments were conducted to probe the phase-separated morphologies of the chiral rod–coil organometallics on a Bruker Nanostar diffractometer. The instrument was equipped with a 3.0 kW X-ray generator using a rotating copper target and operated at 40 kV × 35 mA. The $Cu_{K\alpha}$ line ($\lambda = 0.154$ nm) was applied. The intensity profile was output as the plot of the scattering intensity $I$ versus the scattering vector $q$, $(4\pi/\lambda)\sin(\theta/2)$, in which $\theta$ is the scattering angle. All data were corrected by empty beam scattering, the sensitivity of each pixel of the area detector.

**Molecular simulation**: Mechanisms of self-assembly were studied by considering the interaction of secondary forces through the aid of molecular simulation. The energy minimization of the self-assembly morphology was calculated by using HyperChem 7 with the OPLS force field. Because the OPLS force field was based on a biomolecular database, it should be suitable for use with chiral supramolecular molecules to search stable structures by the Monte Carlo method.

## Acknowledgements

Funding from the National Science Council of Taiwan is gratefully acknowledged (NSC 98-2120-M-007-004). Our appreciation is extended to P.-C. Chao of Regional Instruments Center at NCHU for her help with the TEM experiments.

**Keywords:** amphiphiles · chirality · metallocenes · self-assembly · supramolecular chemistry

[1] a) D. R. Staveren, N. Metzler-Nolte, *Chem. Rev.* **2004**, *104*, 5931–5985; b) V. Bellas, M. Rehahn, *Angew. Chem.* **2007**, *119*, 5174–5197; *Angew. Chem. Int. Ed.* **2007**, *46*, 5082–5104.

[2] a) J. A. Massey, K. Temple, L. Cao, Y. Rharbi, J. Raez, M. A. Winnik, I. Manners, *J. Am. Chem. Soc.* **2000**, *122*, 11577–11584; b) W. Skibar, H. Kopacka, K. Wurst, C. Salzmann, K.-H. Ongania, F. F. Biani, P. Zanello, B. Bildstein, *Organometallics* **2004**, *23*, 1024–1041; c) H. Wang, M. A. Winnik, I. Manners, *Macromolecules* **2007**, *40*, 3784–3789; d) A. P. Soto, I. Manners, *Macromolecules* **2009**, *42*, 40–42.

[3] a) R. G. H. Lammertink, M. A. Hempenius, J. E. v. d. Enk, V. Z.-H. Chan, E. L. Thomas, G. J. Vancso, *Adv. Mater.* **2000**, *12*, 98–103; b) K. Temple, K. Kulbaba, K. N. Power-Billard, I. Manners, K. A.

  

Leach, T. Xu, T. P. Russell, C. J. Hawker, *Adv. Mater.* **2003**, *15*, 297–300; c) S. B. Clendenning, S. Han, N. Coombs, C. Paquet, M. S. Rayat, D. Grozea, P. M. Brodersen, R. N. S. Sodhi, C. M. Yip, Z.-H. Lu, I. Manners, *Adv. Mater.* **2004**, *16*, 291–296; d) C. Hinderling, Y. Keles, T. Stöckli, H. F. Knapp, T. Arcos, P. Oelhafen, I. Korczagin, M. A. Hempenius, G. J. Vancso, R. Pugin, H. Heinzelmann, *Adv. Mater.* **2004**, *16*, 876–879.

[4] a) J. H. Fuhrhop, W. Helfrich, *Chem. Rev.* **1993**, *93*, 1565–1582; b) J. W. Goodby, M. A. Waugh, S. M. Stein, E. Chin, R. Pindak, J. S. Patel, *J. Am. Chem. Soc.* **1989**, *111*, 8119–8125; c) M. S. Spector, R. R. Price, J. M. Schnur, *Adv. Mater.* **1999**, *11*, 337–340; d) J. H. Jung, G. John, K. Yoshida, T. Shimizu, *J. Am. Chem. Soc.* **2002**, *124*, 10674–10675.

[5] a) T. J. Katz, J. Pesti, *J. Am. Chem. Soc.* **1982**, *104*, 346–347; b) R. B. Prince, L. Brunsveld, E. W. Meijer, J. S. Moore, *Angew. Chem.* **2000**, *112*, 234–236; *Angew. Chem. Int. Ed.* **2000**, *39*, 228–230.

[6] R. Oda, I. Huc, M. Schmutz, S. J. Candau, F. C. MacKintosh, *Nature* **1999**, *399*, 566–569.

[7] V. Percec, M. Glodde, T. K. Bera, Y. Miura, I. Shiyanovskaya, K. D. Singer, V. S. K. Balagurusamy, P. A. Heiney, I. Schnell, A. Rapp, H.-W. Spiess, S. D. Hudson, H. Duan, *Nature* **1998**, *391–396*, 384–387.

[8] J. D. Hartgerink, E. Beniash, S. I. Stupp, *Science* **2001**, *294*, 1684–1688.

[9] a) S. Jin, K.-U. Jeong, Y. Tu, M. J. Graham, J. Wang, F. W. Harris, S. Z. D. Cheng, *Macromolecules* **2007**, *40*, 5450–5459; b) E. Yashima, K. Maeda, Y. Okamoto, *Nature* **1999**, *399–402*, 449–451.

[10] a) R.-M. Ho, Y.-W. Chiang, C.-C. Tsai, C.-C. Lin, B.-T. Ko, B.-H. Huang, *J. Am. Chem. Soc.* **2004**, *126*, 2704–2705; b) Y.-W. Chiang, R.-M. Ho, B.-T. Ko, C.-C. Lin, *Angew. Chem.* **2005**, *117*, 8183–8186; *Angew. Chem. Int. Ed.* **2005**, *44*, 7969–7972; c) Y.-W. Chiang, R.-M. Ho, E. L. Thomas, C. Burger, B. S. Hsiao, *Adv. Funct. Mater.* **2009**, *19*, 448–459.

[11] a) J. P. Hill, W. Jin, A. Kosaka, T. Fukushima, H. Ichihara, T. Shimomura, K. Ito, T. Hashizume, N. Ishii, T. Aida, *Science* **2004**, *304*, 1481–1483; b) A. F. Thünemann, S. Kubowicz, C. Burger, M. D. Watson, N. Tchebotareva, K. Mullen, *J. Am. Chem. Soc.* **2003**, *125*, 352–356.

[12] a) C. H. Sung, L. R. Kung, C. S. Hsu, T.-F. Lin, R.-M. Ho, *Chem. Mater.* **2006**, *18*, 352–359; b) T.-F. Lin, R.-M. Ho, C. H. Sung, C. S. Hsu, *Chem. Mater.* **2006**, *18*, 5510–5519; c) T.-F. Lin, R.-M. Ho, C. H. Sung, C. S. Hsu, *Chem. Mater.* **2008**, *20*, 1404–1409.

[13] a) K.-U. Jeong, S. Jin, J. J. Ge, B. S. Knapp, M. J. Graham, J. Ruan, M. Guo, H. Xiong, F. W. Harris, S. Z. D. Cheng, *Chem. Mater.* **2005**, *17*, 2852–2865; b) K.-U. Jeong, B. S. Knapp, J. J. Ge, S. Jin, M. J. Graham, F. W. Harris, S. Z. D. Cheng, *Chem. Mater.* **2006**, *18*, 680–690; c) S.-C. Lin, T.-F. Lin, R.-M. Ho, C.-Y. Chang, C.-S. Hsu, *Adv. Funct. Mater.* **2008**, *18*, 3386–3394, and references therein.

[14] H. Engelkamp, S. Middelbeek, R. J. M. Nolte, *Science* **1999**, *284*, 785–788.

[15] X. Wang, K. Liu, A. C. Arsenault, D. A. Rider, G. A. Ozin, M. A. Winnik, I. Manners, *J. Am. Chem. Soc.* **2007**, *129*, 5630–5639.

[16] a) Y.-F. Chen, I. A. Banerjee, L. Yu, R. Djalali, H. Matsui, *Langmuir* **2004**, *20*, 8409–8413; b) G. Ghini, L. Lascialfari, C. Vinattieri, S. Cicchi, A. Brandi, D. Berti, F. Betti, P. Baglioni, M. Mannini, *Soft Matter* **2009**, *5*, 1863–1869; c) Q. Li, G. Mathur, M. Homsi, S. Surthi, V. Misraa, V. Malinovskii, K.-H. Schweikart, L. Yu, J. S. Lindsey, Z. Liu, R. B. Dabke, A. Yasseri, D. F. Bocian, W. G. Kuhr, *Appl. Phys. Lett.* **2002**, *81*, 1494–1496.

[17] a) A. C. Arsenault, H. Miguez, V. Kitaev, G. A. Oziz, I. Manners, *Adv. Mater.* **2003**, *15*, 503–507; b) A. C. Arsenault, D. P. Puzzo, I. Manners, G. A. Oziz, *Nat. Photonics* **2007**, *1*, 468–472; c) H.-C. Yang, S.-Y. Lin, H.-C. Yang, C.-L. Lin, L. Tsai, S.-L. Huang, I. W.-P. Chen, C.-h. Chen, B.-Y. Jin, T.-Y. Luh, *Angew. Chem.* **2006**, *118*, 740–744; *Angew. Chem. Int. Ed.* **2006**, *45*, 726–730.

Received: March 27, 2010
Published online: June 10, 2010

  